4.3.2 Standard test procedure and interpretation

An example of the results obtained in such a test.

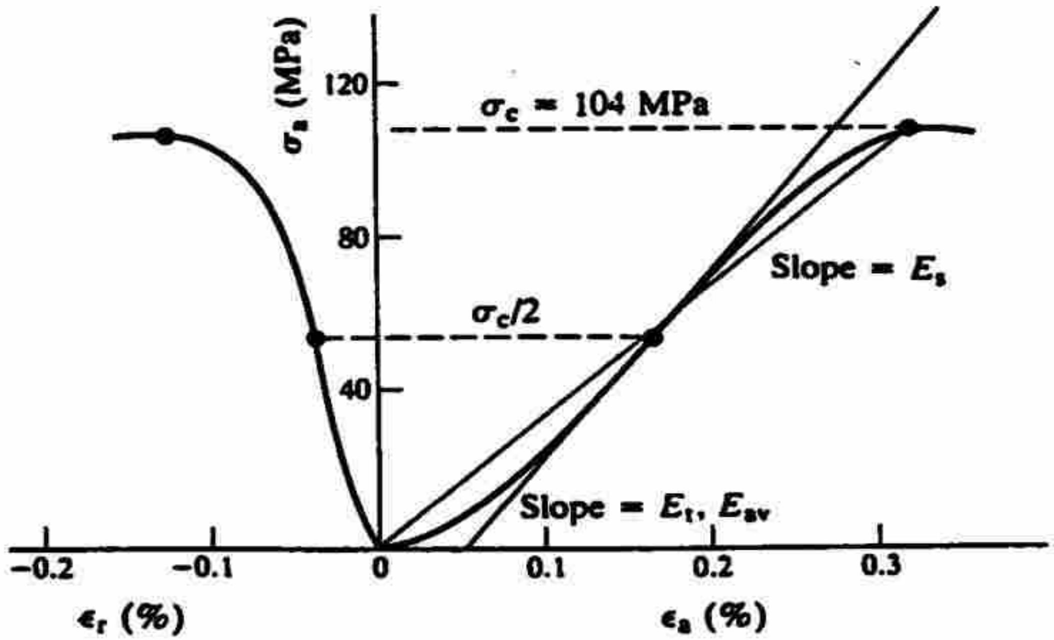

Figure 4.3 Results obtained in a uniaxial compression test on rock.

(a) Tangent Young's modulus, E_t , is the slope of the axial stress-axial strain curve at some fixed percentage, generally 50%, of the peak strength. For E_t = 51.0 GPa.

(b) Average Young's modulus, E_{av} , is the average slope of the more-or-less straight line portion of the axial stress-strain curve. E_{av} = 51.0 GPa.

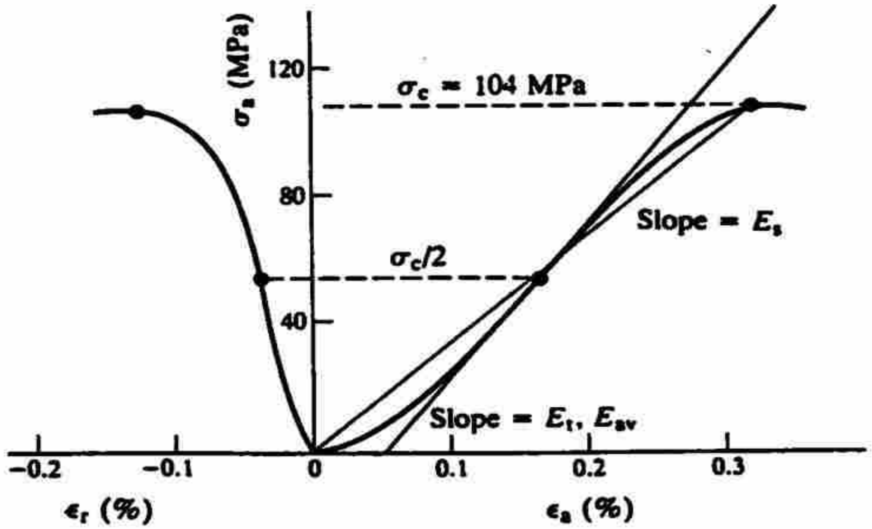

Figure 4.3 Results obtained in a uniaxial compression test on rock.

(c) Secant Young's modulus, E_s , is the slope of a straight line joining the origin of the axial stress-strain curve to a point on the curve at some fixed percentage of the peak strength.

E_s = 32.1 GPa.

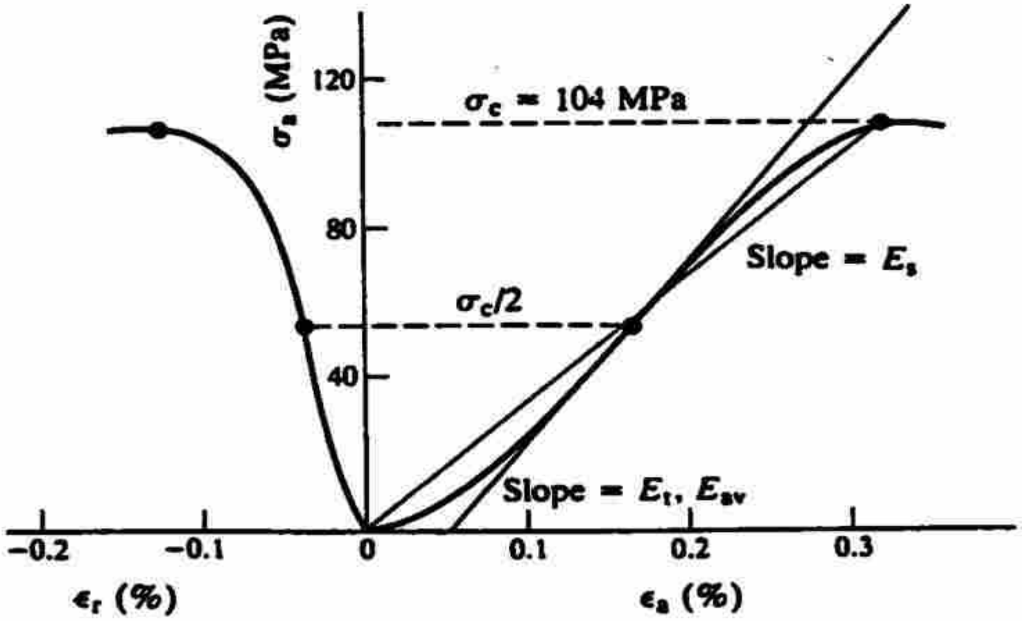

Figure 4.3 Results obtained in a uniaxial compression test on rock.

4.3.2 Standard test procedure and interpretation

Poisson's ratio may be calculated as

$$\upsilon = -\frac{\left(\Delta\sigma_a / \Delta\varepsilon_a\right)}{\left(\Delta\sigma_a / \Delta\varepsilon_r\right)} \qquad \textbf{(4.3)}$$

For the data given in Figure 4.3. the values of corresponding to the values of E_{av} , E_t , and E_s ,

υ calculated above are approximately 0.29, 0.31 and 0.40 respectively.

4.3.2 Standard test procedure and interpretation

Because of the axial symmetry of the specimen, the volumetric strain, ε_v , at any stage of the test can be calculated as

$$\varepsilon_v = \varepsilon_a + 2\varepsilon_r \qquad \textbf{(4.4)}$$

For example, at a stress level of σ_a =80 MPa in Figure 4.3, ε_a =0.220%, ε_r = - 0.055% and ε_v = 0.110%.

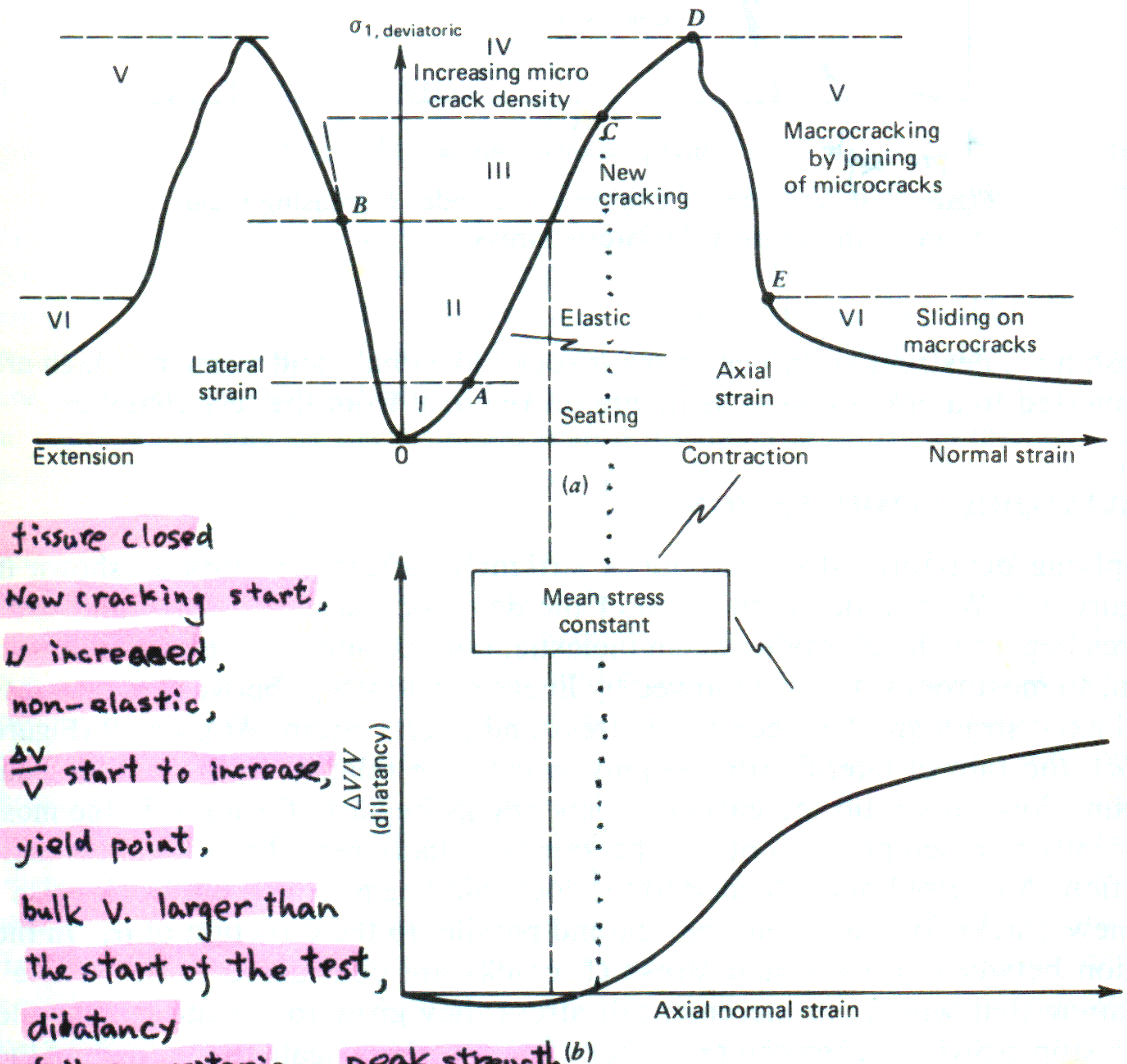

o~A: fissure closed

B: New cracking start,

ν increased,

non-elastic,

$\frac{\Delta V}{V}$ start to increase,

C: yield point,

bulk V. larger than

the start of the test,

dilatancy

D: failure criteria, peak strength

Figure 3.7 Deformation under increasing deviatoric stress, with constant mean stress (hypothetical curves). (*a*) Axial and lateral normal strain with increasing deviatoric axial stress. (*b*) Volumetric strain with increasing axial normal strain (dilatancy).

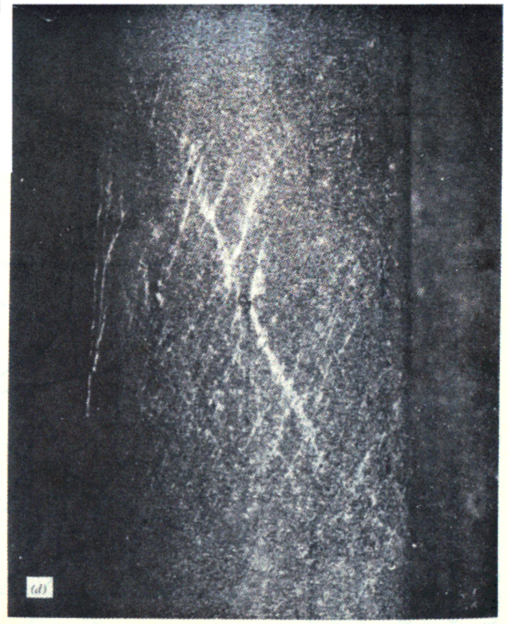

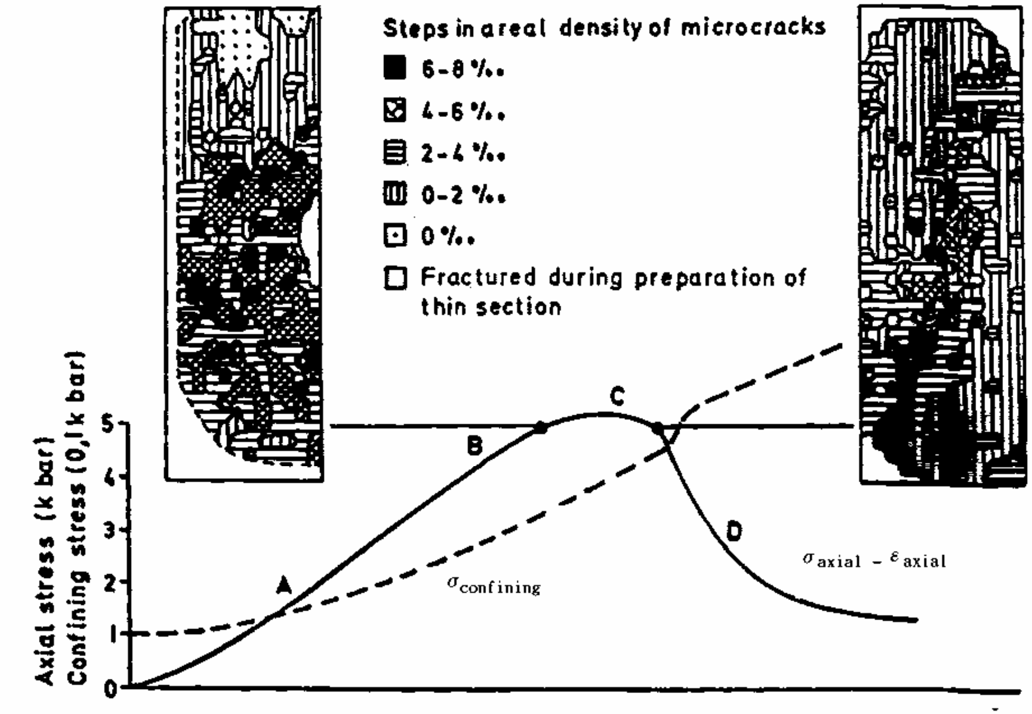

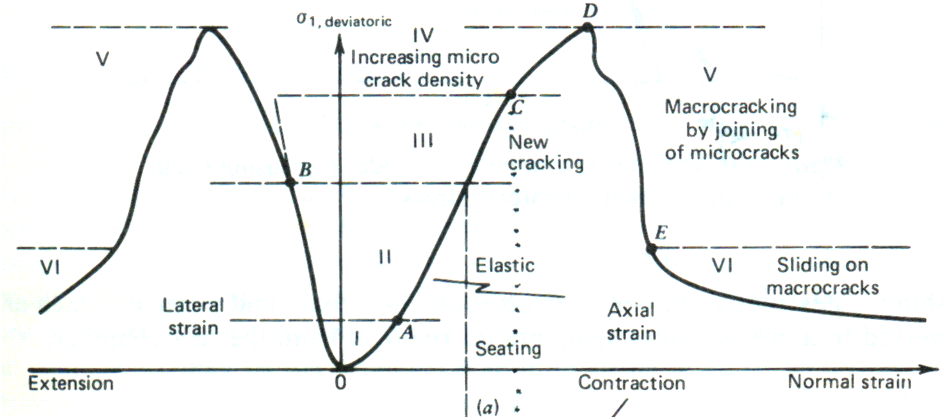

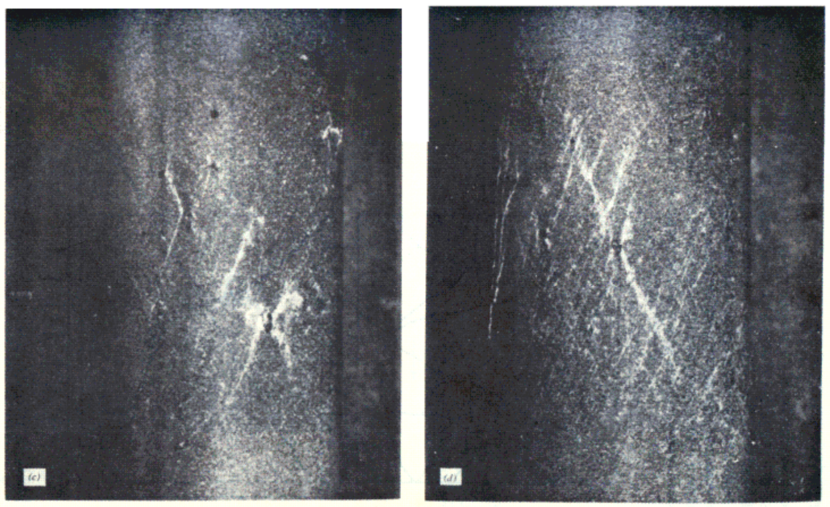

Figure 3.7 Deformation under increasing deviatoric stress, with constant mean stress (hypothetical curves). (*c*) at the peak axial stress; (*d*) just after the peak showing linkup of fractures to form a rupture surface. *c* and *d* Fractures formed in diabase during triaxial compression at 500 psi, reproduced from Wawersik and Brace (1971) with permission.

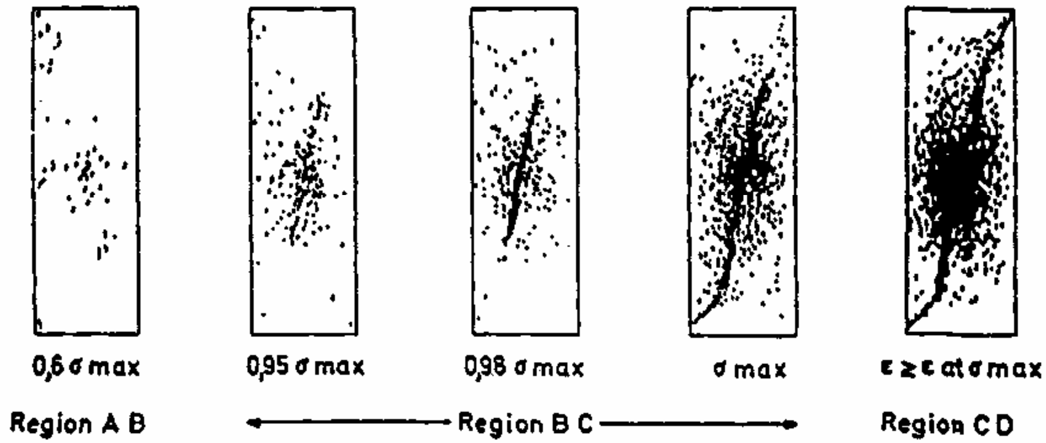

Fig. 4.5.2 A composite representation of the complete stress–strain curve and the incremental radial stress–axial strain curve for a suite of triaxial compression tests done in a stiff-testing machine and in a stiff, sealed triaxial cell, using specimens of argillaceous quartzite prepared from a single piece of rock. The axial sections through specimens stopped at various stages of compression show the structural changes associated with the complete stress–strain curve and associated dilatancy (after Hallbauer *et al.*, 1973).

4.3.3 End effects and the influence of height to diameter ratio

Figure 4.4b illustrates a case in which complete radial restraint occurs at the specimen ends. The result of such restraint is that shear stresses are set up at the specimen-platen contact (Figure 4.4c). This means that the axial stress is not a principal stress and that the stresses within the specimen are not always uniaxial.

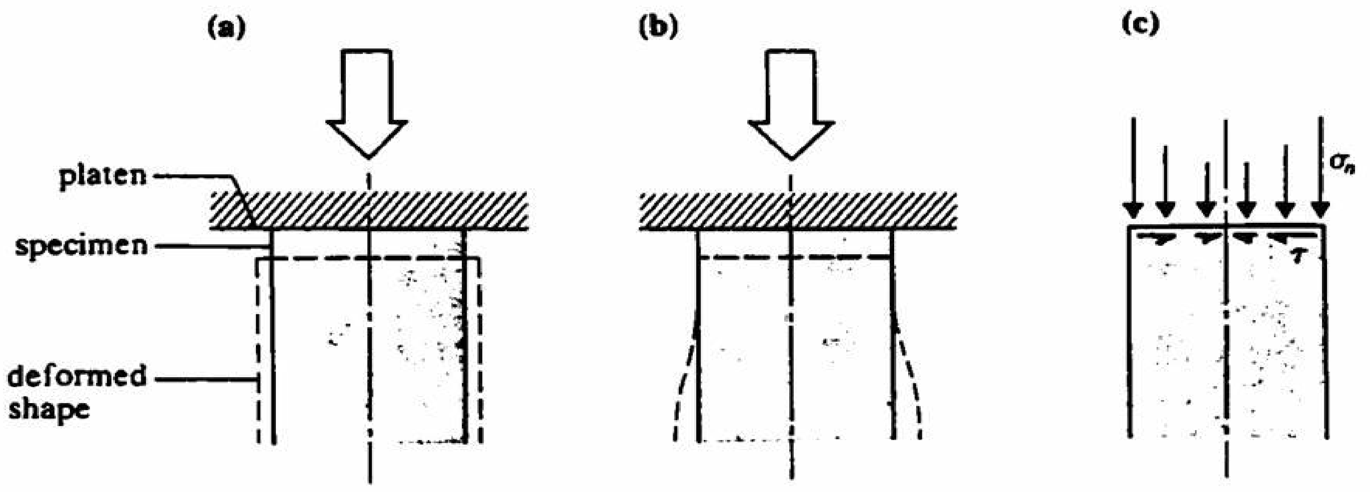

Figure 4.4 Influence of end restraint on stresses and displacements induced in a uniaxial compression test: (a) desired uniform deformation of the specimen; (b) deformation with complete radial restraint at the specimen–platen contact; (c) non-uniform normal stress, σ_n and shear stress, τ, induced at the specimen end as a result of end restraint.

4.3.3 End effects and the influence of height to diameter ratio

As a consequence of these end effects, the stress distribution varies throughout the specimen as a function of specimen geometry.

As the height to diameter (H/D) ratio increases, a greater proportion of the sample volume is subjected to an approximately uniform state of uniaxial stress.

4.3.3 End effects and the influence of height to diameter ratio

Figure 4.5 shows some experimental data which illustrate this effect.

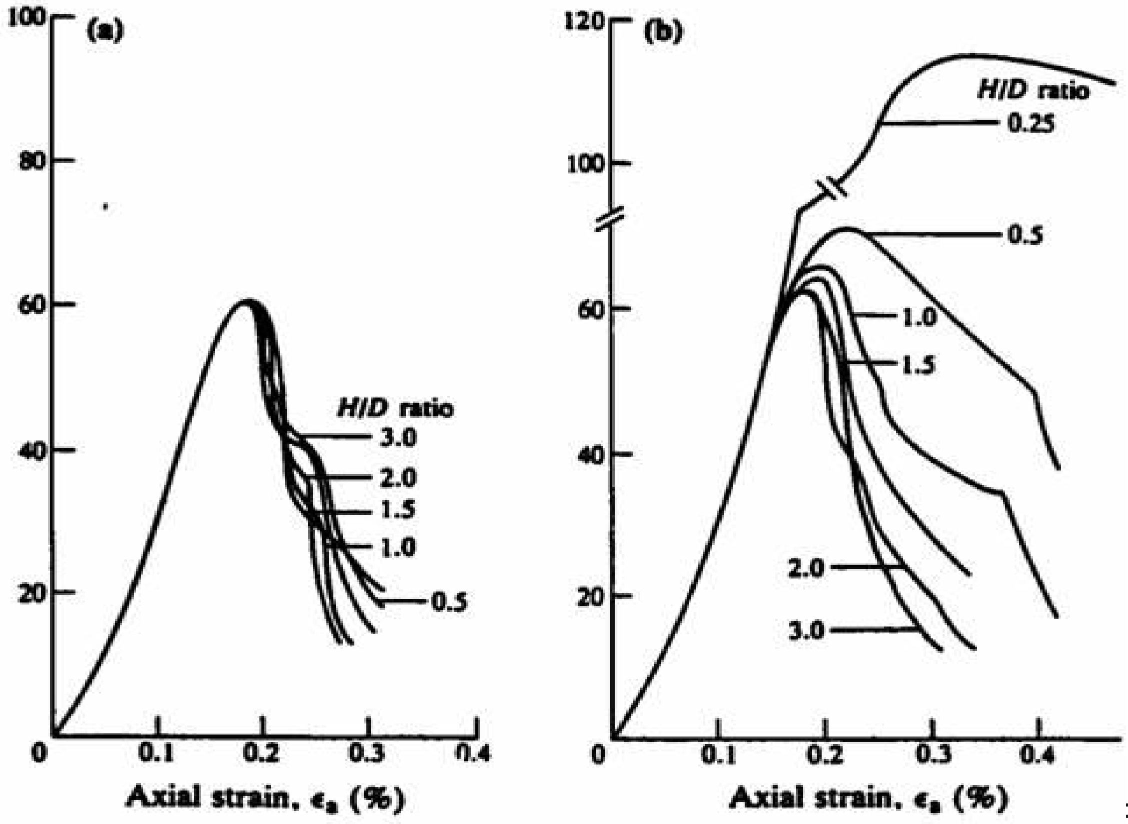

Figure 4.5 Influence of height to diameter (*H/D*) ratio on stress-strain curves obtained in uniaxial compression tests carried out on Wombeyan Marble using (a) brush platens, and (b) solid steel platens (after Brown and Gonano, 1974).

4.3.3 End effects and the influence of height to diameter ratio

When 51 mm diameter specimens of Wombeyan Marble were loaded through 51 mm diameter steel platens, the measured uniaxial compressive strength increased as the H/D ratio was decreased and the shape of the post-peak stress-strain curve became flatter.

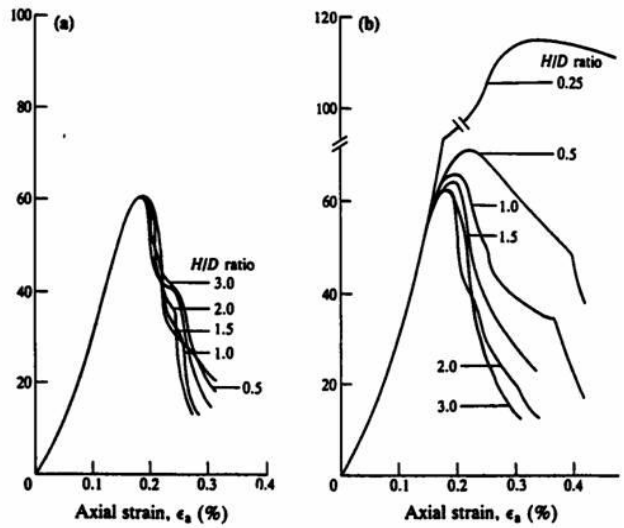

Figure 4.5 Influence of height to diameter (*H/D*) ratio on stress-strain curves obtained in uniaxial compression tests carried out on Wombeyan Marble using (a) brush platens, and (b) solid steel platens (after Brown and Gonano, 1974).

4.3.3 End effects and the influence of height to diameter ratio

When the tests were repeated with 'brush' platens (made from an assembly of 3.2 mm square high-tensile steel pins), lateral deformation of the specimens was not inhibited; similar stress-strain curves were obtained for HID ratios in the range 0.5 to 3.0. However, 'brush' platens were found to be too difficult to prepare and maintain for their use in routine testing to be recommended.

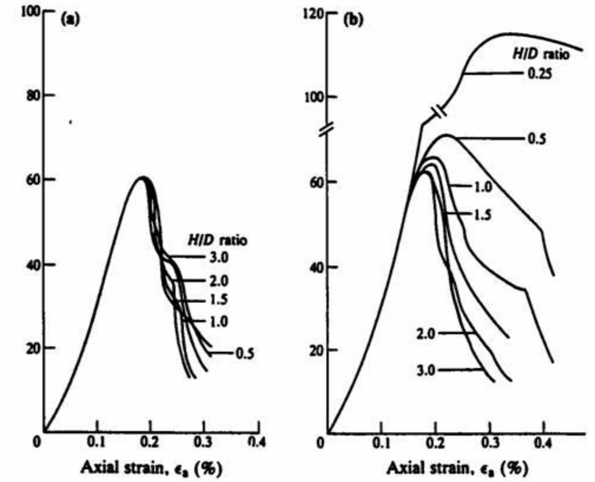

Figure 4.5 Influence of height to diameter (H/D) ratio on stress-strain curves obtained in uniaxial compression tests carried out on Wombeyan Marble using (a) brush platens, and (b) solid steel platens (after Brown and Gonano, 1974).

4.3.3 End effects and the influence of height to diameter ratio

It is tempting to seek to eliminate end effects by treating the specimen-platen interface with a lubricant or by inserting a sheet of soft material between the specimen and the platen. Experience has shown that this can cause lateral tensile stresses to be applied to the specimen by extrusion of the inserts or by fluid.

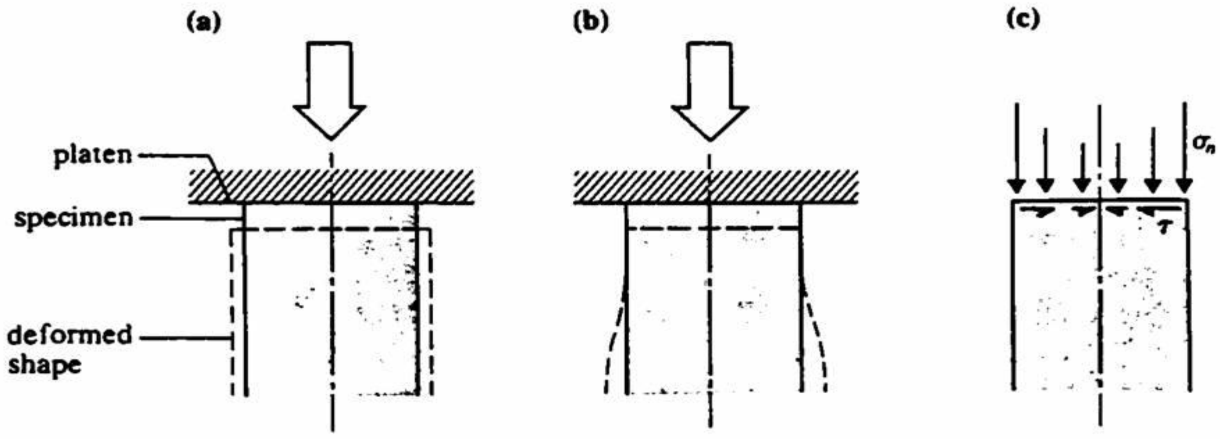

Figure 4.4 Influence of end restraint on stresses and displacements induced in a uniaxial compression test: (a) desired uniform deformation of the specimen; (b) deformation with complete radial restraint at the specimen–platen contact; (c) non-uniform normal stress, σ_n and shear stress, τ, induced at the specimen end as a result of end restraint.

4.3.3 End effects and the influence of height to diameter ratio

For this reason, the ISRM Commission (1979) and other authorities (e.g. Hawkes and Melior, 1970; Jaeger and Cook. 1979) recommend that treatment of the sample ends, other than by machining, be avoided.

4.3.4 Influence of the standard of end preparation

In Figures 4.3 and 4.5, the axial stress-axial strain curves have initial concave upwards sections before they become sensibly linear. This initial portion of the curve is generally said to be associated with 'bedding-down' effects.

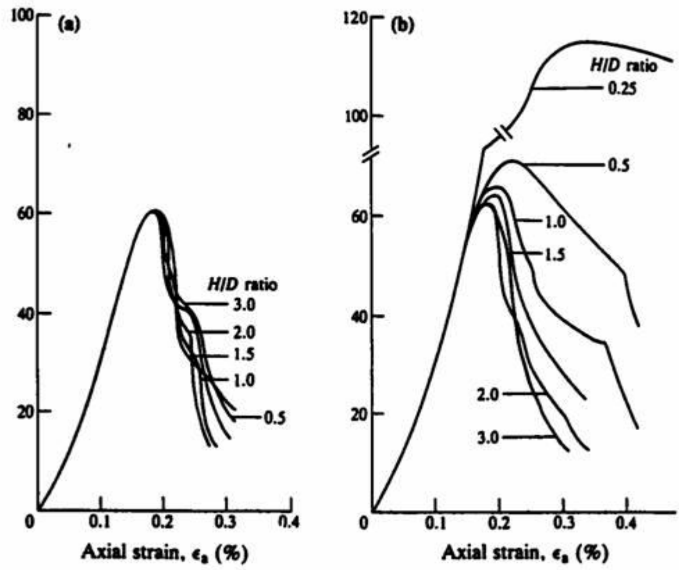

Figure 4.5 Influence of height to diameter (*H/D*) ratio on stress-strain curves obtained in uniaxial compression tests carried out on Wombeyan Marble using (a) brush platens, and (b) solid steel platens (after Brown and Gonano, 1974).

4.3.4 Influence of the standard of end preparation

The extent of this portion of the curve can be greatly reduced by paying careful attention to the flatness and parallelism of the ends of the specimen.

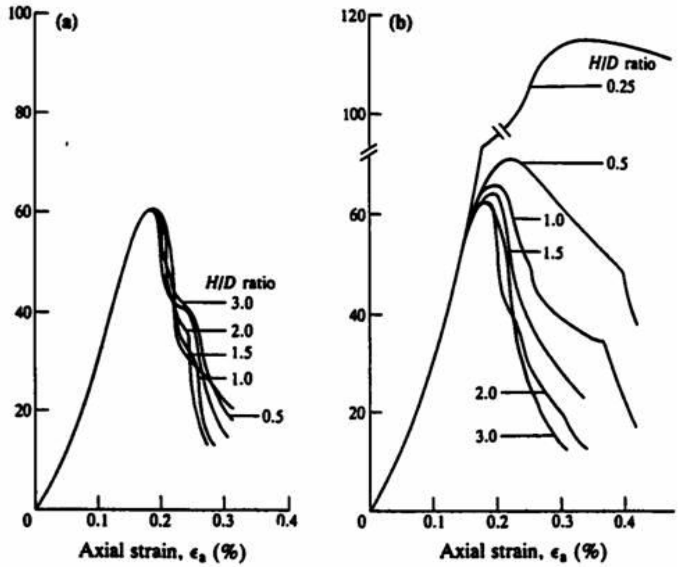

Figure 4.5 Influence of height to diameter (*H/D*) ratio on stress-strain curves obtained in uniaxial compression tests carried out on Wombeyan Marble using (a) brush platens, and (b) solid steel platens (after Brown and Gonano, 1974).

4.3.4 Influence of the standard of end preparation

The ISRM Commission (1979) recommends that in a 50+ mm diameter specimen, the ends should be flat to within 0.02 mm and should not depart from the perpendicular to the specimen axis by more than 0.05 mm.

4.3.4 Influence of the standard of end preparation

Even when spherical seats are provided in the platens, out-of-parallelism of this order can still have a significant influence on the shape of the stress-strain curve, the peak strength.

For research investigations, the authors prepare their 50-55 mm diameter specimens with ends flat and parallel to within 0.01 mm.

4.3.5 Influence of specimen volume

It has often been observed experimentally that, for similar specimen geometry, the uniaxial compressive strength of rock material, σ_c , varies with specimen volume.

Generally, it is observed that σ_c decreases with increasing specimen volume, except at very small specimen sizes where inaccuracy in specimen preparation and surface flaws or contamination may dominate behaviour and cause a strength decrease with decreasing specimen volume.

4.3.5 Influence of specimen volume

This, coupled with the requirement that the specimen diameter should be at least 10 times the size of the largest grain, provides a reason for using specimen diameters of approximately 50 mm in laboratory compression tests.

4.3.5 Influence of specimen volume

Many explanations have been offered for the existence of size effects, but none has gained universal acceptance. A popular approach is to interpret size effects in terms of the distribution of flaws within the material.

4.3.6 Influence of strain rate

The ISRM Commission (1979) recommends that a loading rate of $0.5-1.0\,MPa\ s^{-1}$ be used in uniaxial compression tests. This corresponds to a time to the attainment of peak strength in the order of 5-10 min.

4.3.6 Influence of strain rate

As the arguments presented below show, it is preferable to regard strain or deformation, rather than axial stress or load, as the controlling variable in the compression testing of rock. For this reason, the following discussion will be in terms of axial strain rate, $\dot{\varepsilon}_a$, rather than axial stress rate.

4.3.6 Influence of strain rate

The times to peak strength recommended by the ISRM Commission (1979) correspond to axial strain rates in the order of $10^{-5} - 10^{-4}\ s^{-1}$.

For very fast and very slow strain rates, differences in the observed stress-strain behaviour and peak strengths can become quite marked. However, a change in strain rate from $10^{-8}\ s^{-1}$ to $10^{2}\ s^{-1}$ may only increase the measured uniaxial compressive strength by a factor of about two. Generally, the observed behaviour of rock is not significantly influenced by varying the strain rate within the range that it is convenient to use in quasi-static laboratory compression tests.

4.3.7 Influence of testing machine stiffness

Figure 4.6 illustrates the interaction between a specimen and a conventional testing machine. The specimen and machine are regarded as springs loaded in parallel. The machine is represented by a linear elastic spring of constant longitudinal stiffness, k_m, and the specimen by a non-linear spring of varying stiffness, k_s.

Figure 4.6 Spring analogy illustrating machine–specimen interaction.